Transitions of Saturated Monoacid Triglycerides: Modeling Conformational Change at Glycerol During $\alpha \rightarrow \beta' \rightarrow \beta$ Transformation

J.W. Hagemann* and **J.A. Rothfus**

Biopolymer Research, National Center for Agricultural Utilization Research, U.S. Department of Agriculture, Agricultural Research Service, Peoria, Illinois 61604

The glycerol region geometry of modeled saturated monoacid triglycerides was altered by bond rotations and minor angle distortions to convert theoretical α-forms into bent β'- and β-forms. Direct α to β conversion involves lateral disruption of fatty chain packing to generate side-chain character typical of the β-form. Such disruption, which could contribute to fat bloom, allows additional molecular movement and shifts in molecular mechanics energy (MME) that may approximate thermal changes observed by differential scanning calorimetry during α to β transformations. Energy calculations at 100 points throughout each transformation identified plausible conversion routes. A two-stage conversion, α to either of two stereospecific β'-forms bent at glycerol followed by subsequent conversion to β, showed less chain movement and more favorable MME than direct α to β conversion. The preferred path, based on energy profiles of each conversion, involves a β'-D form and rotation of carbonyl to α-carbon bonds in chain #2 and a side chain (chain #3).

KEY WORDS: Computer modeling, molecular mechanics energy, phase transitions, polymorphism, triglycerides.

Lipids assume different crystal forms *via* multiple melting behavior. This polymorphism is critical to the organized structure and vital activities of biomembranes (1), and it imparts favored texture and other important qualities to processed foods (2).

Though years of research have produced much descriptive information on lipid polymorphism (3,4), mechanisms by which polymorphic effects operate are not well understood (5–7). Detailed knowledge of molecular conformation in monoacid saturated triglycerides is limited to that of the highest-melting β-form polymorph (8), and relatively little is known of molecular motion that occurs during polymorphic transitions.

Nuclear magnetic resonance (NMR) studies (9), which indicate equivalent environments at C_1 and C_3 of glycerol in α- and β'-form saturated triglycerides, are consistent with tuning fork configurations in such molecules (8,10). In β-form triglycerides, however, each glycerol carbon confronts a slightly different environment. There is little or no motion of glycerol carbons in each discrete polymorph, but distinct differences between the three are consistent with bond rotations in the glycerol head group during form transition (9). Data from both NMR (9,11) and differential scanning calorimetry (DSC) (12) studies suggest that constituent atoms lose motion throughout the $\alpha \rightarrow \beta' \rightarrow \beta$ transformation sequence. Some 10 to 30% of an α-form molecule may remain rotationally free, but efficient packing in β-form triglycerides essentially excludes rotational freedom (11,12). It remains to be seen, however, how rotational freedom partitions and affects atomic configuration as energy and motion are removed from a population of molecules undergoing $\alpha \rightarrow \beta$ transformation. Understanding of such processes at the molecular level should lead to effective schemes for selecting polymorphic forms and regulating their transformations. For example, the molecular motion that produces fat bloom, a large solidification expansion that accompanies rapid β-form formation in saturated monoacid triglycerides and certain other fats (13), is especially interesting.

Unfortunately, concentration effects, time resolution, sample dimensions and other complicating factors often obscure the views of polymorphic transitions allowed by conventional instrumentation. To augment such approaches, we have used computational chemistry to probe for details of bond rotations and chain movements that must occur in or near the glycerol region (9) as symmetrical α or β' glycerides convert to unsymmetrical β-form structures. This modeling, performed on single molecules with calculations relative to an arbitrary starting position, leads to plausible schemes that may aid in understanding $\alpha \rightarrow \beta$, $\alpha \rightarrow \beta'$ and $\beta' \rightarrow \beta$ transformations.

EXPERIMENTAL PROCEDURES

Modeling system. The Chem-X molecular modeling system, developed and distributed by Chemical Design Ltd., Oxford, England, is an integrated package of software that can generate atomic coordinates for three-dimensional molecular models from standard bond lengths, angles and torsion angles. Models can be displayed on a graphics terminal and manipulated for viewing from any angle. Molecular geometry can be modified by commands that rotate portions of each molecule about single bonds. Additional commands allow measurements of interatomic distances and angles and the calculation of molecular mechanics energies (MMEs) (14). The Chem-X software was run on a Digital MicroVAX 2000 computer (Digital Equipment Corp., Marlborough, MA) equipped with a Tektronix 4225 high-resolution terminal (Tektronix Inc., Beaverton, OR).

The $\alpha \rightarrow \beta$ conversion parameters. Models of trilaurin were used to investigate changes required to convert a theoretical α-form structure to the β-form known from single-crystal x-ray data (8). The trilaurin α-form was prepared from a previously modeled (10) triarachidin molecule, which can be described as having nonparallel chains, carbonyl right and the same zigzag pattern on chains #1 and #3 [Fig. 1(A) in ref. 10]. Figure 1 shows a portion of the trilaurin molecule and the numbering system used for the atoms. This α-form model was chosen for study because the orientation of its chain #2 carbonyl oxygen resembles that in the known β-form trilaurin.

Images of the α and β molecules were placed on the computer terminal screen simultaneously, and the three glycerol carbons in each molecule were superimposed by adjusting bond lengths and angles in the α-form model. Starting at the glycerol carbons, bonds were rotated in

*To whom correspondence should be addressed at National Center for Agricultural Utilization Research, 1815 North University Street, Peoria, IL 61064.

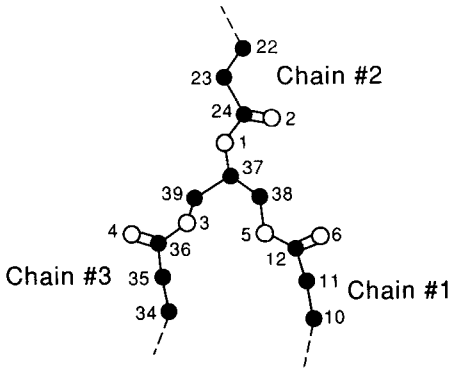

FIG. 1. Chain and atom labeling of abbreviated trilaurin used in phase-transition analyses. Chains are numbered according to Lutton (ref. 15). Carbon atoms are filled circles; oxygen atoms, open circles; hydrogen atoms, not shown.

the α-form molecule until the first moveable atoms beyond the bond being rotated were coincident or nearly so. For example, bond C_{38}-C_{37} was rotated to alight O_5 atoms. This alignment was repeated successively along each chain. To achieve a better fit, other angles in the α-form were also changed to approximate those of the known β-form (8). Parameters used for the α to β conversion are listed in Table 1.

The α→β′ and β′→β conversion. Parameter changes for the α→β′ and β′→β conversions were determined in the same manner as were those for α→β. The α-forms were converted to either of two types of β′-forms bent in the glycerol region, as described previously (16). The two β′-forms are referred to as β′-U (rotations involving chains #1 and #3) and β′-D (rotations involving chain #2) where U (upward) and D (downward) indicate chain direction when the molecule is viewed down the bond from hydrogen to the central carbon of glycerol. For β′→β studies, the starting α-form was first converted to either the U or D form. Parameter changes for α→β′ and β′→β conversions are listed in Table 1.

Phase transitions. Phase transition experiments were performed with a triarachidin model by applying parameter changes determined with the trilaurin model. For discussion purposes, atom numbers that identify particular bond lengths, angles or rotations are identical to those for trilaurin (Fig. 1).

Three different pathways were studied: α→β, α→β′ and β′→β. In each, the total parameter change was divided into 100 steps. At each step, parameters were incremented a portion of their total value, and the MME was calculated to obtain an energy profile for the transition. For α→β

TABLE 1

Molecular Adjustments for Triglyceride Phase Transitions

Parameter modified or operation performed[a]	α→β	α→β′-U	α→β′-D	β′-U→β	β′-D→β
Glycerol Atoms					
C_{37}-C_{38} bond	1.54→1.46 Å	—	—	1.54→1.46 Å	1.54→1.46 Å
C_{37}-C_{39} bond	1.54→1.73 Å	—	—	1.54→1.73 Å	1.54→1.73 Å
∡C_{39}-C_{37}-C_{38}	109.98→117.01°	—	—	109.98→117.01°	109.98→117.01°
Rotate C_{37}-C_{38}	8°	—	—	—	−28°
Rotate C_{37}-C_{39}	−10°	—	—	—	48°
Rotate C_{38}-C_{37}	−7°	—	—	−20°	—
Rotate C_{39}-C_{37}	55°	—	—	62°	—
Chain #1					
∡O_5-C_{38}-C_{37}	110.80→102.77°	—	—	—	110.80→102.77°
Rotate O_5-C_{38}	62°	—	—	96°	69°
Rotate C_{12}-O_5	−35°	−20.50°	—	−5°	−14°
Rotate C_{11}-C_{12}	−95°	172.30°	—	75°	−98°
Rotate C_{10}-C_{11}	−6°	—	—	−5°	—
Chain #2					
∡C_{39}-C_{37}-O_1	107.03→113.34°	—	—	107.03→116.69°	107.03→116.69°
∡C_{38}-C_{37}-O_1	—	—	—	88.62→103.16°	92.20→103.16°
∡C_{23}-C_{24}-O_1	—	—	—	—	116.49→109.30°
∡C_{22}-C_{23}-C_{24}	—	—	—	111.19→113.50°	—
Rotate O_1-C_{37}	43°	—	—	27°	55°
Rotate C_{24}-O_1	60°	—	27°	50°	34°
Rotate C_{23}-C_{24}	32°	—	−83°	48°	118°
Rotate C_{22}-C_{23}	−1°	—	—	20°	2°
Chain #3					
∡C_{36}-O_3-C_{39}	—	—	—	120.35→123.40°	—
∡C_{35}-C_{36}-O_3	109.74→120.24°	—	—	109.74→120.24°	109.74→120.24°
∡C_{34}-C_{35}-C_{36}	109.32→105.17°	—	—	109.32→105.17°	109.32→105.17°
Rotate O_3-C_{39}	−12°	—	—	4°	−17°
Rotate C_{36}-O_3	83°	19.00°	—	56°	85°
Rotate C_{35}-C_{36}	177°	147.60°	—	21°	206°
Rotate C_{34}-C_{35}	104°	—	—	118°	97°
Rotate C_{33}-C_{34}	—	—	—	24°	8°

[a]Refer to Figure 1 for atom numbering system.

conversions, additional experiments involved mathematical adjustments to the step increments of selected parameters to reduce chain movement and to search for additional plausible polymorphs.

Routines for the $\alpha \rightarrow \beta$ conversion were as follows: (i) linear increments of all parameters at each step; (ii) a cosine function for selected parameters to produce larger movements near Step 50; (iii) reversal of the C_{35}–C_{36} bond rotation, −183° rather than 177° (Table 1); and (iv) a gradually increasing increment for the C_{34}–C_{35} bond rotation (17).

RESULTS

Application of conversion parameters given in Table 1 achieved good fit between a converted α-form trilaurin molecule and the β-form trilaurin known from x-ray data (8). The average displacement between corresponding atoms of 18 pairs represented by the atoms in Figure 1 was 0.39 Å. This value approaches the level of uncertainty (±0.1 Å) in the unit cell dimension resultant for β-form trilaurin. Accordingly, to keep computations brief, additional α-form bond lengths and angles were left unadjusted. In effect, the model approximated an average molecule in the population of β-form molecules seen by x-ray.

The largest displacements between the converted α and known β molecules occurred between O_2 and O_6 pairs, 0.87 and 0.96 Å, respectively. Angles that these atoms in the converted α-form molecule made with corresponding atoms in the β molecule, by using coincident carbonyl carbons as the apex, averaged 42.5°, *i.e.*, the angle $O_2(\beta)$=$C_{24}(\beta)$:O_2(converted α) equaled 43.6°. However, angles that the carbonyl oxygens made with chains to which they were bounded, *i.e.*, -C-C=O and O=C-O-, Figure 1, were approximately the same. The greatest difference was a 13° variation at O_6. This means that the carbonyl oxygen possesses some freedom of position for possible packing efficiency or hydrogen bonding and still satisfies bond angle requirements. The average distance between terminal carbon pairs (C_1, C_{13} and C_{25}), not shown in Figure 1, was 0.34 Å.

The $\alpha \rightarrow \beta$ transitions. During this phase of the search for conformational changes that promote glyceride polymorphism (Fig. 2), long hydrocarbon chains were held rigid in extended *trans* configurations to accentuate effects due to bond perturbations in the glycerol region. Examination of all possible *gauche* conformers, which would be appropriate for a realistic picture of molecular motion during polymorphic transformation, proved unnecessary in this initial investigation.

Change from the symmetrical chain configuration in α-form triarachidin to the characteristic β orientation of chain #3 involved the largest bond rotation angles of any transition, notably, the C_{34}–C_{35} and C_{35}–C_{36} bonds (Table 1). This rotation of a rigid chain #3 produced a large outward circular movement in the ±X direction (Fig. 2) during all $\alpha \rightarrow \beta$ conversions that involved linear increments at each step. Some such out-of-plane distortion of chain packing, most likely through *gauche* conformer formation, may accompany the dimensional changes (*e.g.*, fat bloom) exhibited by certain fats in thermally unstable environments. Chains #1 and #2 showed relatively little movement throughout the transition. In the starting

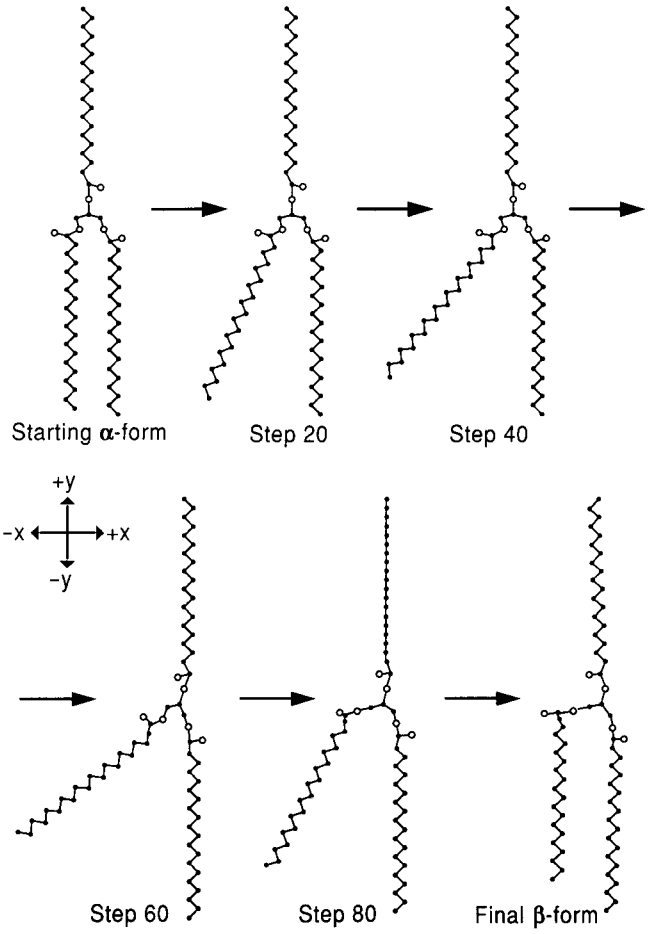

FIG. 2. $\alpha \rightarrow \beta$ Transformation with linear parameter increments at each step.

triarachidin α-form model, chains #1 and #3 were separated by approximately 5 Å. The greatest displacement of chain #3 during the transition occurred near Step 60, in which the terminal carbon atom of chain #3 was 24.9 Å from the nearest carbon atom of chain #1. Views of the molecules in Figure 2 rotated 90° show that displacement in the Z direction was about one-third that in the −X direction.

Minimization of this displacement of chain #3 was attempted in subsequent experiments. By setting the structure at Step 15 and rotating various angles back to their starting positions, it was determined that the C_{36}–O_3, C_{35}–C_{36} and C_{39}–C_{37} rotations were primarily responsible for the outward movement. Use of a cosine expression to assign larger rotation increments to these three bonds during mid-transition allowed effects from other rotations to occur before the large displacement of chain #3. All other rotations were incremented linearly. This adjustment reduced the outward swing of chain #3 (Fig. 2) 0.3 Å, and, as expected, the greatest movement occurred near Step 50.

The best rotation angle for the C_{35}–C_{36} bond was 177°. Reversal of this bond rotation, −183°, produced a chain #3 movement in the +X direction opposite to that of Figure 2. This opposite rotation combined with linearly incremented rotations of the C_{36}–O_3 and C_{39}–C_{37} bonds did produce less chain movement, but it also caused close

approach of chain #3 methylene protons to those of chain #1 near the glycerol region.

Parametric changes listed in Table 1 include what appears to be duplicate bond rotations, *i.e.*, C_{37}–C_{39} and C_{39}–C_{37} during $\alpha \rightarrow \beta$. Replacing these rotations with a single change, 45°, produces a different effect because atoms moved during each individual rotation are connected to the first-named atom. Thus, the C_{37}–C_{39} rotation moves chain #2 while the C_{39}–C_{37} rotation moves chain #3.

Further on-screen monitoring of selected bond rotations suggested that if the C_{34}–C_{35} rotation angle were still relatively small when the C_{35}–C_{36} and C_{36}–O_3 rotations were more than 50% complete, outward movement of chain #3 might be reduced further. Application of an increasing exponential function to the C_{34}–C_{35} bond rotation produced outward movement similar to Figure 2, but it was reduced to 22.0 Å at steps 60, nearly three Å less than the displacement experienced with all-linear increments at each step.

Energy curves for the modeled $\alpha \rightarrow \beta$ transitions are shown in Figure 3. Transition by reverse rotation of C_{35}–C_{36} is not shown because, as mentioned above, it produced extremely high MMEs. All three curves have two energy maxima, but distances between these maxima and their relative heights depend on the pathway. Rotations based on linear and cosine step increments, Figure 3(a) and (b) respectively, both showed maximum energy around Step 50, between 272–273 Kcal or about 14 Kcal higher than the starting α-form. With exponential step increments, Figure 3(c), the first maximum was delayed and lower in magnitude compared to the other transitions. The minima between energy peaks ranged from 266.3 Kcal at Step 67 for the cosine increments to 268.7 Kcal at Step 77 for the exponential increments. While the linear and exponential expressions produced an initial rise in energy followed by a short plateau, an initial decrease of 1.3 Kcal was observed at Step 7 when using the cosine expression. Overall, interactions throughout the exponential and cosine-adjusted paths made these routes favorable energetically compared to the linear-increment path. Compared by integration, the exponential and cosine paths involved 7 and 12% less energy, respectively, than the linear path.

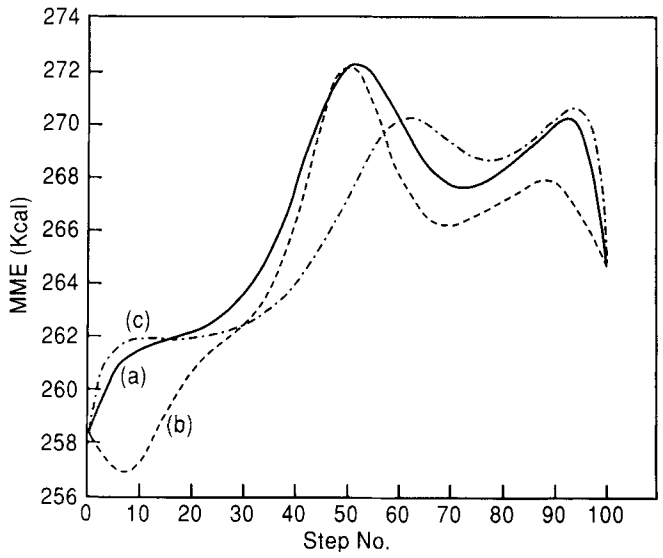

FIG. 3. Molecular mechanics energy (MME) profiles for $\alpha \rightarrow \beta$ conversions: (a) linear parameter increments for each change at each step, (b) cosine function modulation of C_{39}–C_{37}, C_{36}–O_3 and C_{35}–C_{36} bond rotations at each step; linear increments for all other parameter changes, (c) increasing exponential function for the C_{34}–C_{35} bond rotation at each step. Linear increments for all other parameter changes.

The $\alpha \rightarrow \beta'$ transitions. Transformation of α-form triglycerides to β'-form need not involve bond rotations within the glycerol moiety itself (Table 1). The β'-form molecules bent in the glycerol region (16) were achieved readily through either of two routes by selective bond rotations at carbonyl carbons, as illustrated in Figure 4. Conversion of α to either β'-U or β'-D entailed some chain movement out of a plane defined by the original α-form molecule.

Synchronous movement of chains #1 and #3 formed β'-U *via* a path (Fig. 5) that included an initial 3-Kcal dip

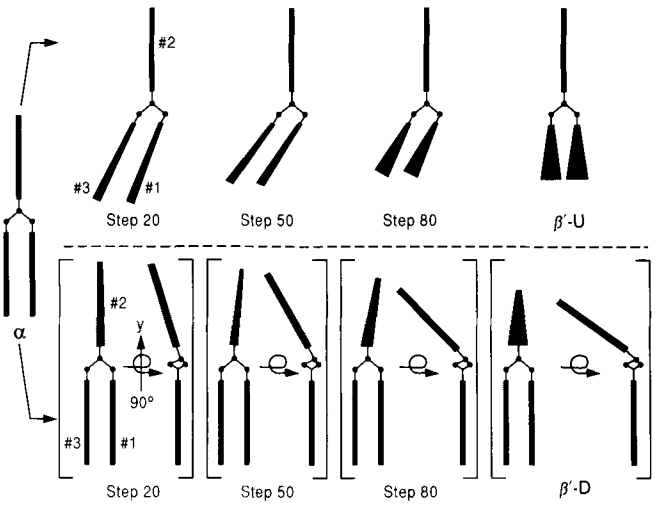

FIG. 4. Schematic illustrations of $\alpha \rightarrow \beta'$-U and $\alpha \rightarrow \beta'$-D transformations. Line width in β'-U structures implies projection upward from plane of figure and the reverse for β'-D structures.

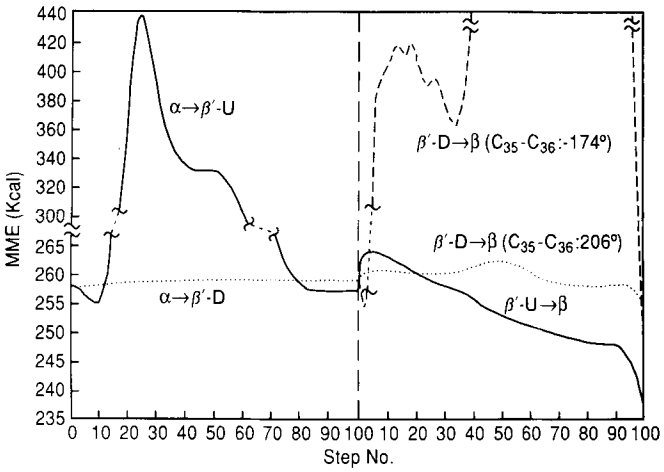

FIG. 5. Molecular mechanics energy (MME) profiles for $\alpha \rightarrow \beta'$-U/$\beta'$-D and β'-U/β'-D→β transformations.

similar to the adjustment observed in the cosine-modulated α to β transformations (Fig. 3). This minimum at Step 9 was followed by an energy maximum of 437 Kcal at Step 24, which was 179 Kcal higher than the starting α-form energy level. A level region around Step 45 in the energy trace suggests a stable structure, but the molecule length at this step was between values reported for α and β' forms of triarachidin by Lutton and Fehl (18). Beyond step 85, the curve was level indicating equivalent energy structures.

Only a 0.6-Kcal increase in energy was found in the $\alpha \rightarrow \beta'$-D conversion (Fig. 5). Chain movement in the $\pm$X direction, the axis of greatest displacement in previous conversions, was negligible, and conversion was accomplished merely by straight-forward collapse in the Z direction.

The $\beta' \rightarrow \beta$ transitions. Transformation of either β'-U or β'-D triarachidin to the β-form, in which chain #3 assumes a characteristic side-chain orientation, required essentially the same number of molecular adjustments as were necessary in the $\alpha \rightarrow \beta$ transition (Table 1). The transformation also required reversal of the β' molecular bend at glycerol. Both $\beta' \rightarrow \beta$ transitions involved chain movements, but movements of markedly different type.

The β'-U$\rightarrow\beta$ transformation involved greater dislocation of chain #1 than chain #3, but β'-D$\rightarrow\beta$ was the reverse (Fig. 6), rather like $\alpha \rightarrow \beta$. The β'-D$\rightarrow\beta$ transition also resembled $\alpha \rightarrow \beta$ in that rotation of the C_{35}-C_{36} bond (Table 1) produced circular motion of chain #3 in the +X direction, close approach of some atoms and high MME values throughout a large portion of the conversion (Fig. 5). In contrast, MME for β'-U$\rightarrow\beta$ rose slightly, 6.5 Kcal, then declined gradually to that for the final β structure. When the direction of C_{35}-C_{36} rotation was reversed in the β'-D$\rightarrow\beta$ conversion, 206° *vs.* −174°, the high-energy region was eliminated, and the energy trace for the transition consisted of two relatively flat areas separated by an energy barrier of approximately 2.5 Kcal at Step 50 (Fig. 5).

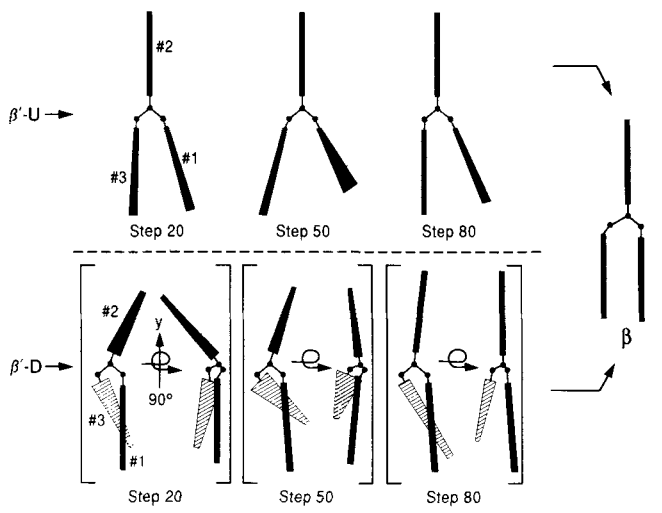

FIG. 6. Schematic illustration of β'-U$\rightarrow\beta$ and β'-D$\rightarrow\beta$ transformations. Line width in β'-U structures implies projection upward from plane of figure and the reverse for β'-D structures.

DISCUSSION

The expansion of solidifying fats, fat bloom, is a well-known phenomenon often observed when saturated even triglycerides, and some fully hydrogenated fats, are held at temperatures that promote transition to higher melting forms, *i.e.,* temperatures near α-form melting points, which depend on fatty acid chainlength (12). Molecular origins of this behavior, however, remain obscure due to limits on data that correlate dimensional change with composition and tempering conditions.

Bailey and Singleton (19), who measured the expansion of a series of solid and liquid triglycerides dilatometrically, actually reported a decrease in specific volume and a contraction of tristearin throughout $\alpha \rightarrow \beta' \rightarrow \beta$ transitions. It is significant in terms of our studies that they observed the largest contraction of tristearin during the $\beta' \rightarrow \beta$ transition.

Hvolby (13), however, classified tristearin as an "expanding" fat and reported that completely hydrogenated soybean oil, upon voluntary cooling, expanded violently with a volume change equivalent to the creation of 35% vol/vol cavities in the original fat. He concluded that an "expanding" fat does so when it crystallizes at "moderate velocity." Practical problems that Hvolby experienced in dealing with dimensionally unstable hydrogenated soybean oil were also encountered later by Dafler (20). Both Hvolby and Dafler speculate that fat bloom is driven by relief of strain in an anisotropic population of solidified triglycerides such that the solid expands more in one direction than in any other, perhaps through distortion of relatively stable layers by adjacent layers of molecules that are undergoing conformational change.

Expansion during polymorphic transition apparently occurs by change in lateral packing of triglycerides, because x-ray diffraction patterns attributable to such packing change the most during phase transitions of bloom-prone fats (20).

Experimental data thus identify three important elements of triglyceride polymorphism pertinent to fat bloom. The process: (i) is driven thermodynamically by transformation of the initial solid to an energetically favored form with higher crystal density; (ii) proceeds *via* a kinetically regulated sequence; and (iii) involves directioned dislocations. Furthermore, recent elegant work by Kellens *et al.* (21) demonstrates that few of the molecules in a transposing sample are liquid. In data from their time-resolved x-ray diffraction studies, phase transitions of tripalmitin appear to occur *via* rapid, perhaps concerted, disruptions of the crystal lattice. Accordingly, it was reassuring to find that models for the α-forms of trilaurin and triarachidin convert easily to the corresponding β'-forms by as few as two bond rotations (Table 1). Such rotations, propagated throughout a population of molecules simultaneously or sequentially, would allow rapid phase transition with minimal dislocation of carbon chain interactions.

Analysis of the models further suggests, however, that transitions to the highest-melting, β-form, conformations require somewhat greater disruption of the previous crystal structure. This result is consistent with x-ray data that show selective improvement in crystal order along the b axis during development of the β phase (21).

The α→β transitions. Modeling of solid fats, activated sufficiently to disrupt the lateral packing of adjacent triglyceride molecules, suggests that out-of-plane chain movement, as represented in Figure 2, could contribute to the directional expansion of fat bloom. Such movement would also allow lattice adjustments that produce the large transformation exotherm observed between α- and β-forms during DSC (12,22).

The amount of chain movement shown in Figure 2, which would more than double sample volume of the triglyceride, is an obvious exaggeration. It serves here, however, to emphasize the importance of spatial and temporal contexts in which conformational adjustments must occur if specific transformations are to be achieved. For example, delay of the C_{34}-C_{35} bond rotation relative to rotations in C_{35}-C_{36} and C_{36}-O_3 modulated the outward displacement of chain #3 and reduced the energy barrier encountered at mid-transition in the α→β conversion, Figure 3(c). Exponential modulation of the C_{34}-C_{35} bond rotation reduced MME for the α→β conversion slightly compared to that for rotation incremented linearly. Cosine modulation of other bonds, Figure 3(b), produced even greater reduction overall. These results hint at energetically favored conversion paths that remain proper subjects for future modeling, which should also consider molecular population effects.

The temporal sensitivity of polymorphic transitions is further illustrated by comparing MME tracings in Figure 3. Cosine modulation of C_{39}-C_{37}, C_{36}-O_3 and C_{35}-C_{36} bond rotations [Fig. 3(b)] reduced MME initially at Step 7. This could easily be due to structural refinement of the type that gives rise to multiple α-forms observed in DSC of long-chain triglycerides (12). At Step 7, the starting α-form model has undergone little change, but that which has occurred apparently predisposes the system to a path involving less interaction near Step 90.

Energy maxima at Steps 50 and 60 (Fig. 3) occur as chain #3 reaches its optimum outward position (Fig. 2) and the nonbonded energy term of MME exhibits a maximum. Views of the molecule in Figure 2 rotated 90° about the Y-axis show that chain #3 is aligned and coplanar with chain #1. Views of the molecule around Step 90 show that chain #3 is near its final β-form position but still at an angle with the linear chain #1 and #2 alignment. The minimum between energy peaks, Steps 68 to 77, shows chain #3 at a slight angle to chains #1 and #2, and likely results from more efficient proton interactions between chains #1 and #3.

Data in Figure 3 further show the final β-form energy to be 6 Kcal higher than the starting α-form. This apparent contradiction to the concept that α→β conversion leads to a lower energy form (23) results from two facts: (i) subtle changes in proton alignment between chains #1 and #3 can affect MME and (ii) the triglyceride molecules, after completion of the 100-step transition, were not optimized to achieve lower energies. Subsequent energy plots in this report, which reflect slight unobservable differences in bond lengths and angles, do show a lower β-form energy than that in Figure 3. It should also be pointed out that the energy calculated for individual molecules will be different than that calculated for the same molecule in a multiple molecule environment, where the terraced end-group packing of the β-form (8) is preferred to the hydrocarbon end-group packing of α-forms (24).

The α→β′ transitions. Historically, paths to β′-forms have been somewhat controversial, even though generally accepted concepts of triglyceride polymorphism include a β′ intermediate among the progression of forms associated with the multiple melting points of saturated triglycerides (12,23,25–28). Hernqvist and Larsson (28) have stated that α must be passed to get β′, and that β′ must be present to get β. But nearly 30 years ago, Chapman (29) reported that β′ is produced by cooling the liquid melt to a temperature several degrees above the melting point of α. More recent work on triglyceride polymorphism with DSC, positron lifetime measurements and time-resolved x-ray diffraction (21,30,31) concludes that the β′-form can only be crystallized from the isotropic melt, yet it reports a fleeting presence of β′ during the transition of α to β (21). Questions of kinetics are central to this controversy. The β′-form has often been trapped without knowledge of conformational changes that produce the form or allow its conversion to another. Our results suggest a middle ground between the differing viewpoints.

Our interest in the α→β′ transition is based on evidence that the post-melt triglyceride liquid state contains β-like dimeric units (28,32) and on the corresponding likelihood of tuning fork structures in liquid near the α-form melting point. Experiments on the α→β′ transition thus extend logically to the formation of β′ from the liquid state.

Substantially different chain movements are involved in the conversion of an α-form triglyceride to either β′-U or β′-D (Fig. 4). For β′-U, chains #1 and #3 undergo circular movement that requires equal but opposite movement in adjacent molecules. This is difficult to accomplish without chain overlap or close approach of atoms. Formation of β′-D, however, merely involves a straight-forward bending of chain #2 without appreciable outward swing of the chain.

In both cases, if chain movement is accompanied by tilting of the molecule, as described by Larsson for diglycerides (33), adjacent chain contact is minimized. Symmetrical chain movement and synchronous tilting of molcules eliminate packing strain of the type encountered in the direct α→β transition (Fig. 2). From an energy standpoint, the α→β′-D transition is preferred (Fig. 5) as MME increases only slightly during this conversion.

Computation thus leads to the conviction that α→β′ conversions can occur quite rapidly and give rise to molecules bent at glycerol with a conformation, β′-D (Fig. 4), somewhat different from Larsson's proposed β′-form (33), which involves changes in chains #1 and #3, as in β′-U.

The β′→β transitions. Side-chain character in chain #3, the distinctive feature of β-form triglycerides, can be generated readily from β′ forms by routes that resemble either α→β′ or α→β. Energy considerations (Fig. 5) and chain movement (Fig. 6) favor β′-U→β. The change in MME for this transition is not inconsistent with observed exotherms for α→β conversions (12). Furthermore, as shown in Figure 6, chains #2 and #3 undergo relatively little movement.

However, if the position of chain #2 relative to glycerol is critical and β′-U→β transformation must follow from the β′-D form generated in α→β′, then the favored route would involve chain movement more like that seen during α→β (Fig. 2). As with α→β, this transition requires a large positive rotation of the C_{35}-C_{36} bond to prevent unfavorable chain interaction (Fig. 6) and prohibitive

transition MME values (Fig. 5). The modeled $\alpha \rightarrow \beta$ type transformation of the β'-D form incorporates lateral disruption of the crystal lattice, as seen by x-ray (21). It also reduces the mid-transition energy barrier, which would make $\beta' \rightarrow \beta$ conversion more likely, as is typical of even-chainlength saturated triglycerides.

Overall, the modeled conversions indicate that even-chainlength β-form triglycerides can form from α-form solid or α-like liquid by a two-step process that is consistent with x-ray data (21) and the conclusions of both Dafler (20) and Walker (30). The process would involve a simple collapse of the molecule as described by Larsson (33), followed by a return to the normal position for chain #2 and the formation of the side-chain orientation for chain #3.

Our report intentionally omits discussion of a number of plausible alternative mechanisms discarded when their exploration led to undesirable interactions and energy levels, or when conditions analogous to the described paths were encountered. Similarly, we draw no conclusions about conformational sequences for odd-chainlength triglycerides, which may be quite different from those followed by even-chainlength molecules.

REFERENCES

1. Thompson, G.A., *The Regulation of Membrane Lipid Metabolism*, CRC Press, Inc., Boca Raton, 1980.
2. D'Souza, V., J.M. deMan and L. deMan, *J. Am. Oil Chem. Soc. 67*:835 (1990).
3. Small, D.M. (ed.), *The Physical Chemistry of Lipids: from Alkanes to Phospholipids*, Plenum Press, New York, 1986.
4. Garti, N., and K. Sato (eds.), *Crystallization and Polymorphism of Fats and Fatty Acids*, Marcel Dekker Inc., New York, 1988.
5. Macdonald, A.G., *Biochem. J. 256*:313 (1988).
6. Macdonald, A.G., *Biochim. Biophys. Acta 1031*:291 (1990).
7. Smith, R.L., and E. Oldfield, *Science 225*:280 (1984).
8. Larsson, K., *Ark. Kemi 23*:1 (1965).
9. Bociek, S.M., S. Ablett and I.T. Norton, *J. Am. Oil Chem. Soc. 62*:1261 (1985).
10. Hagemann, J.W., and J.A. Rothfus, *Ibid. 60*:1308 (1983).
11. Norton, I.T., C.D. Lee-Tuffnell, S. Ablett and S.M. Bociek, *Ibid. 62*:1237 (1987).
12. Hagemann, J.W., and J.A. Rothfus, *Ibid. 60*:1123 (1983).
13. Hvolby, A., *Ibid. 51*:50 (1974).
14. Allinger, N.L., *Adv. Phys. Org. Chem. 13*:1 (1976).
15. Lutton, E.S., *J. Am. Oil Chem. Soc. 48*:245 (1971).
16. Hagemann, J.W., and J.A. Rothfus, *Ibid. 65*:638 (1988).
17. Hagemann, J.W., and J.A. Rothfus, *Ibid. 69*:429 (1992).
18. Lutton, E.S., and A.J. Fehl, *Lipids 5*:90 (1970).
19. Bailey, A.E., and W.S. Singleton, *Oil and Soap 22*:265 (1945).
20. Dafler, J.R., *J. Am. Oil Chem. Soc. 54*:249 (1977).
21. Kellens, M., W. Meeussen, C. Riekel and H. Reynaers, *Chem. Phys. Lipids 52*:79 (1990).
22. Hagemann, J.W., W.H. Tallent and K.E. Kolb, *J. Am. Oil Chem. Soc. 49*:118 (1972).
23. Whittam, J.H., and H.L. Rosano, *Ibid. 52*:128 (1975).
24. Hernqvist, L., *Fette Seifen Anstrichm. 86*:297 (1984).
25. Larsson, K., *Ark. Kemi 23*:35 (1965).
26. Hoerr, C.W., and F.R. Paulicka, *J. Am. Oil Chem. Soc. 45*:793 (1968).
27. Lutton, E.S., *Ibid. 49*:1 (1972).
28. Hernqvist, L., and K. Larsson, *Fette Seifen Anstrichm. 84*:349 (1982).
29. Chapman, D., *Chem. Rev. 62*:433 (1962).
30. Walker, W.W., *J. Am. Oil Chem. Soc. 64*:754 (1987).
31. Kellens, M., W. Meeussen and H. Reynaers, *Chem. Phys. Lipids 55*:163 (1990).
32. Larsson, K., *Fette Seifen Anstrichm. 74*:136 (1972).
33. Larsson, K., *Chemica Scripta 1*:21 (1971).

[Received July 20, 1992; accepted December 16, 1992]